Available online at www.sciencedirect.com
ScienceDirect
Surface Science 600 (2006) 4190–4194
SURFACE SCIENCE
www.elsevier.com/locate/susc

Morphological and magnetic properties of $Ge/Mn_xGe_{1-x}/Ge(001)2\times1$ diluted magnetic semiconductor

P. De Padova [a,*], A. Generosi [a], B. Paci [a], V. Rossi Albertini [a], P. Perfetti [a], C. Quaresima [a], B. Olivieri [b], M.C. Richter [c], O. Heckmann [c], F. D'Orazio [d], F. Lucari [d], K. Hricovini [c]

[a] CNR-ISM, via Fosso del Cavaliere, 00133 Roma, Italy
[b] CNR-ISAC, via Fosso del Cavaliere, 00133 Roma, Italy
[c] LMPS, Université de Cergy-Pontoise, Neuville/Oise, 95031 Cergy-Pontoise, France
[d] INFM-Dipartimento di Fisica, Università di L'Aquila, Via Vetoio-Coppito, I-67010 L'Aquila, Italy

Available online 19 May 2006

Abstract

We studied morphological and magnetic properties of $Ge/Mn_xGe_{1-x}/Ge(001)2\times1$, $x = 0.02$–0.04. Several Mn_xGe_{1-x} alloys were grown on $Ge(001)2\times1$ by molecular beam epitaxy, as a function of substrate temperature and Mn concentration. The samples were characterized in situ by RHEED, and ex situ by energy dispersive X-ray reflectivity (EDXR) and magneto-optical Kerr effect, (MOKE). From RHEED analysis we found an optimal growth temperature $T_{epi} = 523$ K to achieve 2D epitaxial Mn_xGe_{1-x} ($x = 0.02$–0.04) alloy on a Ge(001) substrate. X-ray reflectivity measurements provided: the film roughness, the Mn_xGe_{1-x} scattering length density, and the average thickness for all samples. MOKE analysis showed ferromagnetism with Curie temperature $T_C = 270$ K for samples grown at $T_{epi} = 523$ K.

Keywords: DMS; RHEED; EDXR; MOKE

1. Introduction

Spin-based electronics uses the transport properties induced by the electron spin. This approach opens a way to a new generation of devices combining standard microelectronics with spin-dependent effects that derive from the interaction between the spin of the carriers and the magnetic properties of the material [1]. Doping of semiconductors by magnetic ions can produce magnetic semiconductors [2,3] having transport properties dependent on spin-carriers. For this reason, diluted magnetic semiconductors (DMS), which are semiconductors doped by low concentration of magnetic elements, have attracted a lot of interest during the last years.

The magnetic properties of DMS systems depend on numerous parameters such as crystallographic structure, cell strain, impurities concentration, and distance between magnetic atoms. Begqvist et al. [4] have calculated the interatomic exchange interactions in DMS using a first principles theory, and then simulated the Curie temperature (T_C) using a Heisenberg Hamiltonian with magnetic atoms distributed randomly. They demonstrated that the magnetic properties of DMS are dominated by short-range interatomic exchange interactions that have strong directional dependence. They suggest that the magnetic ordering of these materials is heavily influenced by magnetic percolation and that the measured T_C should be very sensitive to details in the sample preparation. Calculations of

* Corresponding author. Tel.: +39 06 49934144; fax: +39 06 49934153.
E-mail address: depadova@ism.cnr.it (P. De Padova).

0039-6028/$ - see front matter © 2006 Elsevier B.V. All rights reserved.
doi:10.1016/j.susc.2006.02.071

ferromagnetism in zinc-blend (and/or diamond) structure DMS has been recently reported by Dietl [5]. They showed T_C evaluation above 100 K for several DMS.

The Mn–Ge system could be a good candidate for DMS. Park et al. [6] have demonstrated ferromagnetic order on Mn_xGe_{1-x} samples obtained by epitaxial MBE growth, with T_C ranging between 25 and 116 K. When the growth temperature of Mn_xGe_{1-x} is above 70 °C, bulk phase precipitates such as FM $Mn_{11}Ge_8$, Mn_5Ge_3, Mn_5Ge, with T_C near room temperature, were observed [6–8].

It is still not clear if the ferromagnetism comes from DMSs or from magnetic precipitates. Recently, Kang et al. [9] investigated the chemical distribution and the local electronic structure of $Mn_{0.06}Ge_{0.94}$ single crystals by scanning photoelectron spectroscopy (SPEM), X-ray absorption spectroscopy (XAS), and photoemission spectroscopy (PES). They found that the DMS sample was not uniform, but formed by stripe-shape microstructures, which arise from the chemical phase separation of the Mn-rich and Mn-depleted phases, and suggested that the observed ferromagnetism in Mn_xGe_{1-x} arise from phase-separated Mn-rich phase.

In this paper we report a study of structural and magnetic properties of Mn_xGe_{1-x} films with $x = 0.02$ and $x = 0.04$, grown by molecular beam epitaxy (MBE) on Ge(0 0 1) substrates. The epitaxial growth was investigated in situ by reflection high energy electron diffraction (RHEED), and ex situ by energy dispersive X-ray reflectivity (EDXR). Roughness, thickness and scattering length density (SLD) in alloys have been obtained ex situ by EDXR. Ex situ magneto-optical Kerr effect (MOKE) measurements have been used to explore the magnetic properties of the Mn_xGe_{1-x} alloys.

2. Experimental

The clean Ge(0 0 1)2×1 surface was obtained by annealing the sample at about 1100 K by resistive heating, assuring that the pressure remained below 2×10^{-10} mbar during the heating. Several Mn_xGe_{1-x} alloys ($0.01 < x < 0.04$) were grown on the Ge(0 0 1)2×1 surface by co-evaporating Mn and Ge at low growth rate, by MBE Knudsen cell sources keeping the substrate temperature in the range from RT to 580 K. The sample temperature was measured by an infrared pyrometer, and the film thickness by a quartz microbalance. In order to perform ex situ measurements, a thin Ge layer covered the surface of the samples. The energy dispersive reflectometer used consists of a non-commercial instrument equipped with a water cooled X-ray W anode tube (Philips, model PW2214/20) supplied with 58 kV and 30 mA and with an EG&G ultra pure Ge solid state detector (SSD), cooled by an electro-mechanical refrigerator (X-cooler) and connected to an integrated spectroscopy amplifier-multi channel analyzer system (92 X spectrum master). The measurements were carried out in the reflection geometry at very low reflection angle in stationary condition of the apparatus, since in EDXR no movement is required [10,11] to collect the reflection profiles [12,13].

MOKE hysteresis loops were measured in a magnetic field up to 0.56 T in both polar and longitudinal geometries, at various temperatures between 13 K and RT, using s-polarized radiation ($\lambda = 1.6$ μm) incident on the film surface at an angle of 45°.

3. Results and discussion

3.1. RHEED

Series of Mn_xGe_{1-x} were grown by MBE on Ge(0 0 1)2×1 by varying the substrate temperature (T_s) from RT to 580 K, and the Mn concentration x from 0.01 to 0.04. RHEED patterns were used to qualitatively measure the morphological properties of the surface samples, in order to determine the optimal temperature, called in the following epitaxial temperature T_{epi}, which gives the layer-by-layer (2D) growth. All RHEED patterns were taken with a primary energy $E = 12$ keV along the [0 1 1] azimuth.

Fig. 1 reports two selected RHEED patterns of 255 Å $Mn_{0.02}Ge_{0.98}$/Ge(0 0 1)2×1, and of 401 Å $Mn_{0.04}Ge_{0.96}$/

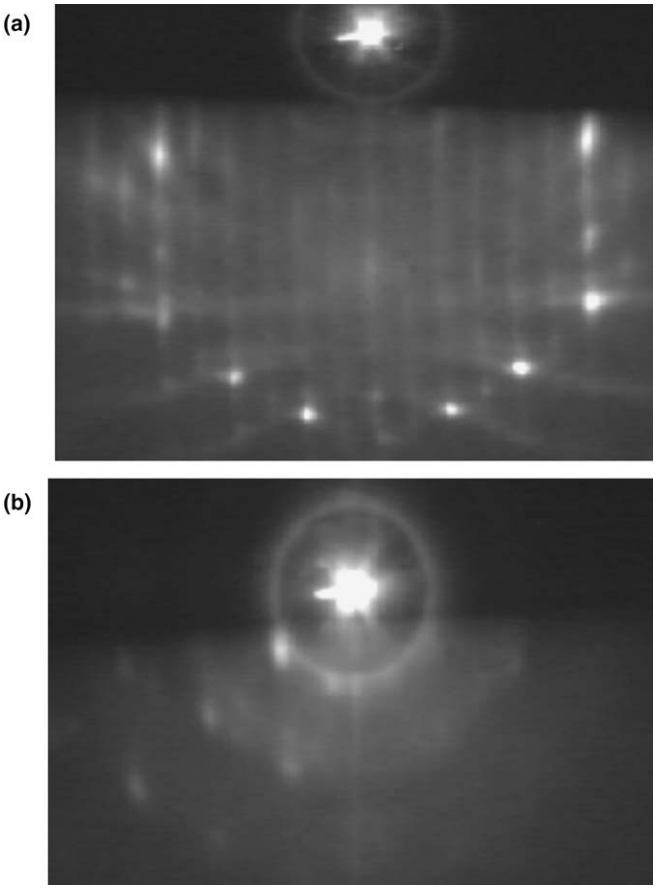

Fig. 1. RHEED patterns along the [0 1 1] azimuth on: (a) Ge/$Mn_{0.04}Ge_{0.96}$/Ge(0 0 1)2×1 grown at 523 K; (b) Ge/$Mn_{0.02}Ge_{0.98}$/Ge(0 0 1)2×1 grown at RT.

Ge(0 0 1)2 × 1 films grown keeping the substrates at 523 K and RT, respectively.

The RHEED pattern of Fig. 1(a) shows streaky fundamental and half-order diffraction features, which indicate a 2 × 1 reconstructed surface [14]. This pattern is similar to that obtained on Ge(0 0 1)2 × 1 clean surface, and shows that the epitaxial growth of $Mn_{0.02}Ge_{0.98}$ alloy on Ge(0 0 1) takes place in 2D modality. On the contrary, RHEED pattern of Fig. 1(b) shows spotty-like structures. These structures are due to bulk scattering of the grazing electron beam from islands of Mn_xGe_{1-x} Mn-rich, or surface asperities formed at RT. At substrate temperature of 523 K for all Mn $0.01 < x < 0.04$ concentration, the RHEED patterns of Mn_xGe_{1-x}/Ge(0 0 1) exhibit features similar to that showed in Fig. 1(a). For temperatures lower than 523 K and Mn concentration $x = 0.01$, 0.015 and 0.02, (1 × 1) unreconstructed or amorphous Mn_xGe_{1-x} films are obtained.

So, these results indicate that for Mn concentrations $0.01 < x < 0.04$, epitaxial growth is obtained around T_{epi} temperature. MBE growth is controlled mainly by parameters like evaporation flux rates and substrate temperature, which affect the surface atoms mobility. When the growth rate R is low (in our case $R = 4$ Å/min), the change on the growth modality can be mostly ascribed to the effect of the substrate temperature. As the growth temperature is lowered, the adatoms surface diffusion is reduced. If new atoms impinge the surface before the previous atoms have formed an ordered layer, they bury the imperfect overlayer and the disorder increases as deposition goes on. Single crystalline growth occurs at a temperature around T_{epi}.

As measured by RHEED pattern, disordered (or amorphous) growth with decreased fractional-order spots takes place below T_{epi}, with (1 × 1) unreconstructed pattern for Mn concentration $x = 0.02$, and formation of islands for $x = 0.04$. This behavior is often observed for homoepitaxial MBE growth. In the regime of low Mn concentration, we can qualitatively consider Mn_xGe_{1-x}/Ge(0 0 1) to be a homoepitaxial growth, similar to Ge/Ge(0 0 1), or Si/Si(0 0 1).

de Jong et al. [15] observed a (1 × 1) LEED pattern of Si/Si(0 0 1) films thinner than 4 nm grown at RT, and Jona [16] reported a (1 × 1) pattern of a 10 nm thick layer of Si/Si(0 0 1) deposited below T_{epi}. The temperature-morphology map for Ge(0 0 1) homoepitaxy is reported in Ref. [17]. The diagram in [17] shows the growth modality of MBE films as a function of substrate temperature and film thickness. In the thickness range 100–500 Å and temperature range 373–523 K layer-by-layer growth is found. Decrease of the temperature leads to the formation of a mounded morphology [18], followed by a transition to amorphous growth at the lowest temperatures.

Our T_{epi} is in good agreement with the value reported by Aarts et al. [19] in Ge/Ge(0 0 1). The authors in [19] followed the Ge homoepitaxy growth by RHEED oscillations and photoemission, and found that around RT the half-order spots in the diffraction pattern disappear within a few layers, and the integral-order (1 × 1) becomes broader and weaker but is still faintly visible after growth of about 50 layers.

3.2. EDXR

The reflectivity patterns, as a function of the radiation wave number k, are the result of the interference of the X-ray beam reflected at the air–film and film–substrate interfaces [20]. They are characterized by a critical value k_c so that for $k < k_c$, the X-ray radiation impinging on the sample is totally reflected, while when $k \approx k_c$ the radiation starts penetrating the sample and, as soon as $k > k_c$, the reflectivity decays more than exponentially with a roughly sinusoidal modulation of the reflected wave amplitude. The position of the critical edge ($k = k_c$) depends on the material density, while the surface roughness (defined as the variance from the average thickness) mainly influences the decay of the reflectivity for $k > k_c$. The wavelength of the sinusoidal modulation of the reflectivity is inversely related to the film thickness. Once the normalization of the reflectivity spectra with respect to the spectral distribution of the primary beam is accomplished, the Parrat model [21–23] for the reflectivity of a film on a substrate was used to fit the experimental data. The general expression for the reflected intensity depends on the SLD, average thickness and surface roughness of the film [24,25].

The fit of the reflectivity spectra using five free parameters, one to normalize the observed intensities, the others to obtain films average thickness, films roughness, and the Mn_xGe_{1-x} scattering length density. The determined average thicknesses are consistent with the values predicted by the known deposition conditions. We only used as free parameter the roughness of the Mn_xGe_{1-x}/air, because that one of the Mn_xGe_{1-x}/substrate interface is considered negligible. Moreover the Ge capping layer is not detectable considering the k^{-1} range explored in the measurement, and then it is not considered in the fitting.

From the fitting procedure the SLD of the Mn_xGe_{1-x} are deduced. The most precise procedure to determine the SLD values from reflectivity measurements, performed in the energy dispersive mode, is to collect several patterns at different angles, each one giving a SLD value. The true SLD is obtained by extrapolating each curve at energy = 0 keV. The measurements should be normalized for geometry-induced intensity variation with angle caused by incident beam [26]. In our case, the reflectivity measurements were performed not varying the geometry, thus not requiring such normalization. Furthermore, since the experimental geometry remains unchanged (beam dimension, sample position, angle and energy), the extrapolation procedure described above was not necessary, since, in the present case, the final goal was a comparison among the electron densities values.

The reflectivity profiles together with their fits of the Ge/$Ge_{0.98}Mn_{0.02}$/Ge(0 0 1) films, grown at RT, at 423 K and at

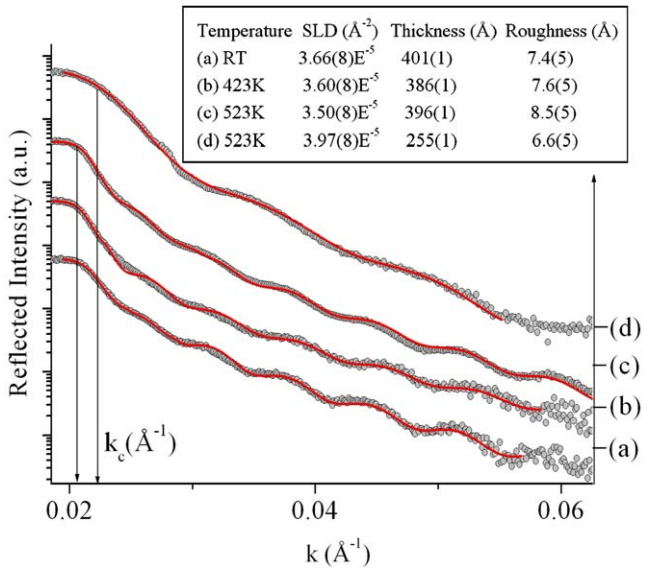

Fig. 2. EDXR spectra on: Ge/$Mn_{0.02}Ge_{0.98}$/Ge for samples grown at (a) RT, (b) 423 K, (c) 523 K and (d) Ge/$Mn_{0.04}Ge_{0.96}$/Ge grown at 523 K. The continuous lines are the fits according to the Parratt model. The arrows indicate the positions of the total reflection edges k_c.

523 K, and Ge/$Ge_{0.96}Mn_{0.04}$/Ge(0 0 1) grown at 523 K are shown in Fig. 2(a)–(d). Despite the low optical contrast between the film and the substrate for all samples, the modulation produced by the interference of the two beams reflected at the film surface and at the interface are visible. The Parratt fit parameters of the data are reported in Fig. 2. Considering the two films grown at 523 K, but with different Mn contribution, the SLD values are $\rho_{film(c)} = 3.97(8)E{-}5$ and $\rho_{film(d)} = 3.50(8)E{-}5$. These SLD values do not correspond neither to pure homogeneous Mn–Ge alloy, nor to pure MnGe precipitates, but probably to a combination of two contributions. Further analysis, such as transmission electron microscopy and X-ray absorption spectroscopy, are in progress to elucidate this point.

3.3. MOKE

We investigated the magnetic properties of all Ge/Mn_xGe_{1-x}/Ge(0 0 1) films by MOKE measurements. We found a magnetic signal only on the samples grown at the higher temperature.

Polar geometry (H perpendicular to the plane) was used for a detailed investigation, since it provides higher Kerr rotations by typically one order of magnitude with respect to the longitudinal geometry (H parallel to the plane). In Fig. 3(a) we report the remanence of the Kerr rotation as a function of temperature in the range of 13–300 K collected on Mn_xGe_{1-x}/Ge(0 0 1)2×1 with $x = 0.04$ grown at $T = 523$ K, while Fig. 3(b) shows the ferromagnetic hysteresis loop collected at $T = 13$ K. From Fig. 3, we derive the Curie temperature $T_C \approx 270$ K. This value can be considered the highest values reported up to now in literature [6,26–28]. As described in the introduction, Park et al. [6] found $T_C = 116$ K on MBE DMS Mn_xGe_{1-x} samples grown at temperature around 343 K. They pointed out that higher temperatures could drive the formation of Mn-rich precipitates. Recently, Kang et al. [9] suggested that the magnetic properties of DMS $Ge_{0.94}Mn_{0.06}$ alloy comes from stripe-shape Mn-rich microstructures chemically separated by a Mn-depleted phase, which constitutes most of the sample. From our RHEED, and EDXR results, we cannot exclude a Mn-rich phase due to microscopic MnGe precipitates, which could be responsible of the observed ferromagnetism.

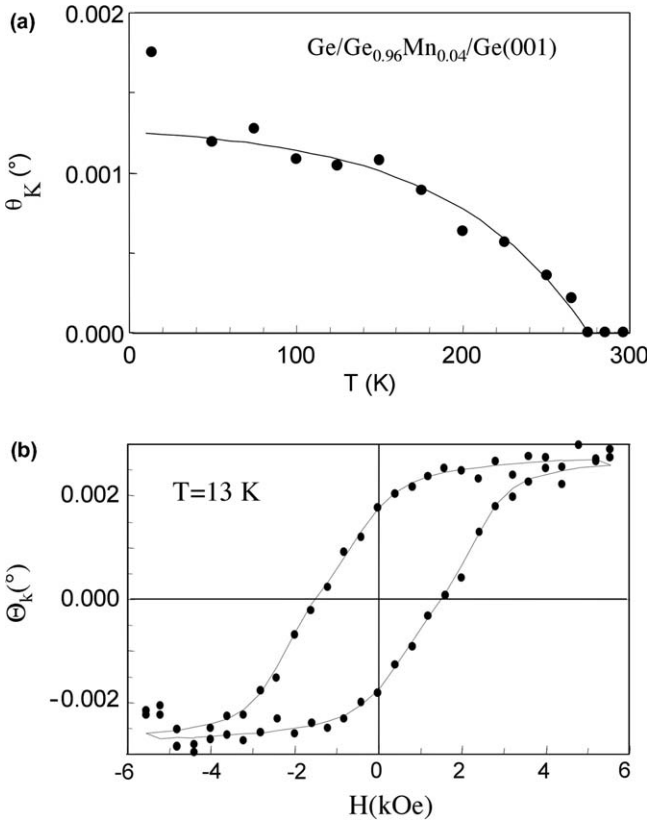

Fig. 3. (a) Kerr rotation performed on Ge/$Mn_{0.04}Ge_{0.96}$/Ge(0 0 1) grown at 523 K. The full circles represent the experimental values, whereas the line is a guide to the eye. (b) Hysteresis loop obtained at 13 K.

Disordered or islanded growth may contain Mn–Mn clusters, which destroy the ferromagnetism as they have antiferromagnetic properties.

4. Conclusions

We have reported the structural and magnetic properties of Ge/Mn_xGe_{1-x}/Ge(0 0 1)2×1 alloys, with $x = 0.02$, 0.04, obtained from RHEED, EDXR and MOKE measurements. From RHEED patterns we have obtained $T_{epi} = 523$ K for 2D epitaxial growth, while from EDXR measurements we have confirmed the films average thickness. MOKE measurements have shown that only Ge/Mn_xGe_{1-x}/Ge(0 0 1)2×1 growth at T_{epi} have ferromagnetic properties with $T_C \approx 270$ K.

Acknowledgments

The authors are grateful to S. Priori and M. Capozi for their appreciable technical assistance. This work was supported by the Italian MIUR (FISR and FIRB projects).

References

[1] T. Dietl, H. Ohno, F. Matsukura, J. Cibert, D. Ferrand, Science 287 (2000) 1019.
[2] K. Hricovini, P. De Padova, C. Quaresima, P. Perfetti, R. Brochier, C. Richter, V. Ilakovac, O. Heckmann, L. Lechevallier, P. Bencok, P. Le Fevre, C. Teodorescu, Appl. Surf. Sci. 212 (2003) 17.
[3] C. Richter, P. De Padova, C. Quaresima, P. Perfetti, R. Brochier, V. Ilakovac, O. Heckmann, L. Lechevallier, M. Zerrouki, P. Le Fevre, C. Teodorescu, C.S. Fadley, N. Hamdan, K. Hricovini, J. Alloys Compd. 362 (2004) 41.
[4] L. Begqvist, O. Eriksson, J. Kudrnovsky, V. Drchal, P. Korzhavji, I. Turek, Phys. Rev. Lett. 93 (2004) 137202-1.
[5] T. Dietl, Phys. Rev. B 63 (2001) 195205.
[6] Y.D. Park, A.T. Hanbicki, S.C. Erwin, C.S. Hellberg, J.M. Sullivan, J.E. Mattson, T.F. Ambrose, A. Wilson, G. Spanos, B.T. Jonker, Science (2002) 295.
[7] S. Cho, S. Choi, S.C. Hong, Phys. Rev. B 66 (2002) 033303.
[8] R. Gunnella, L. Morresi, N. Pinto, R. Murri, L. Ottaviano, M. Passacantando, F. D'Orazion, F. Lucari, Surf. Sci. 577 (2005) 22.
[9] J.-S. Kang, G. Kim, S.C. Wi, S.S. Lee, S. Choi, Sunglae Cho, S.W. Han, K.H. Kim, H.J. Song, H.J. Shin, A. Sekiyama, S. Kasai, S. Suga, B.I. Min, Phys. Rev. Lett. 94 (2005) 147202.
[10] R. Felici, The Rigaku J. 12 (1995) 1.
[11] S.J. Roser, R. Felici, A. Englesham, Langmuir 10 (1994) 3853.
[12] R. Caminiti, V. Rossi Albertini, Int. Rev. Phys. Chem. 18 (1999) 263.
[13] R. Felici, F. Cilloco, R. Caminiti, C. Sadun, V. Rossi, Patent No. RM 93 A 000410, Italy, 1993.
[14] Y. Enta, S. Suzuki, S. Kono, Phys. Rev. Lett. 65 (1990) 2704; R.A. Wolkow, Phys. Rev. Lett. 68 (1992) 2636; E. Fontes, J.R. Patel, F. Comin, Phys. Rev. Lett. 70 (1993) 2790.
[15] T. de Jong, W.A.S. Douma, L. Smit, V.V. Korablev, F.W. Saris, J. Vac. Sci. Technol. B 1 (1983) 888.
[16] F. Jona, Appl. Phys. Lett. 9 (1966) 235.
[17] J.P. Leonard, B. Shin, J.W. McCamy, M.J. Aziz, Mat. Res. Soc. Symp. Proc. 749 (2003) W.16.11.1.
[18] J.E. Van Nostrand, S.J. Chey, M.-A. Hasan, D.G. Cahill, J.E. Greene, Phys. Rev. Lett. 74 (1995) 1127.
[19] J. Aarts, A.-J. Hoeven, P.K. Larsen, J. Vac. Sci. Technol. A 6 (1998) 60.
[20] R.W. James, The Optical Principles of the Diffraction of X-ray, OX BOW Press, Woodbridge, CT, 1982.
[21] L.G. Parratt, Phys. Rev. 95 (1954) 359.
[22] Penfold, Thomas, J. Phys. C 2 (1990) 1369.
[23] M. Mangiantini, R. Felici, Vuoto 23 (1994) 17.
[24] X.L. Zhou, S.H. Chen, Phys. Rep. 257 (1995) 224.
[25] L. Nevot, Croce, Phys. Appl. 15 (1980) 761.
[26] D. Windover, T.-M. Lu, S.L. Lee, A. Kumar, H. Bakhru, C. Jin, W. Lee, Appl. Phys. Lett. 76 (2000) 158.
[27] F. D'Orazio, F. Lucari, M. Passacantando, P. Picozzi, S. Santucci, A. Verna, IEEE Trans. Magn. 38 (2002) 2856.
[28] F. Dorazio, F. Lucari, N. Pinto, L. Morresi, R. Murri, J. Magn. Magn. Mater. 272–276 (2004) 2006.